Comparison of absolute spectral irradiance responsivity measurement techniques using wavelength-tunable lasers

Ville Ahtee,[1,2,*] Steven W. Brown,[3] Thomas C. Larason,[3] Keith R. Lykke,[3] Erkki Ikonen,[1,2] and Mart Noorma[1,3]

[1]Metrology Research Institute, Helsinki University of Technology (TKK), P.O. Box 3000, FI-02015 TKK, Finland
[2]Centre for Metrology and Accreditation (MIKES), P.O. Box 9, FI-02151 Espoo, Finland
[3]National Institute of Standards and Technology (NIST), Gaithersburg, Maryland 20899, USA

*Corresponding author: ville.ahtee@tkk.fi

Received 19 December 2006; revised 23 February 2007; accepted 26 February 2007; posted 2 March 2007 (Doc. ID 78288); published 20 June 2007

Independent methods for measuring the absolute spectral irradiance responsivity of detectors have been compared between the calibration facilities at two national metrology institutes, the Helsinki University of Technology (TKK), Finland, and the National Institute of Standards and Technology (NIST). The emphasis is on the comparison of two different techniques for generating a uniform irradiance at a reference plane using wavelength-tunable lasers. At TKK's Laser Scanning Facility (LSF) the irradiance is generated by raster scanning a single collimated laser beam, while at the NIST facility for Spectral Irradiance and Radiance Responsivity Calibrations with Uniform Sources (SIRCUS), lasers are introduced into integrating spheres to generate a uniform irradiance at a reference plane. The laser-based irradiance responsivity results are compared to a traditional lamp-monochromator-based irradiance responsivity calibration obtained at the NIST Spectral Comparator Facility (SCF). A narrowband filter radiometer with a 24 nm bandwidth and an effective band-center wavelength of 801 nm was used as the artifact. The results of the comparison between the different facilities, reported for the first time in the near-infrared wavelength range, demonstrate agreement at the uncertainty level of less than 0.1%. This result has significant implications in radiation thermometry and in photometry as well as in radiometry.

OCIS codes: 120.3940, 120.5630.

1. Introduction

Many national metrology institutes (NMIs) have adopted the practice of realizing an absolute detector-based spectral irradiance scale [1–5] using cryogenic radiometers as the primary standard because it offers a relatively short traceability chain and low uncertainties compared with the traditional source-based method. Several different calibration techniques for the absolute spectral irradiance responsivity of filter radiometers are commonly in use [6–10]. The uncertainties achievable in spectral responsivity measurements based on traditional approaches using a lamp and a monochromator as a radiation source are limited by the low radiant flux available and the relatively broad spectral width of the source [6,7]. Laser-based methods overcome these limitations as they offer orders of magnitude more power and, for cw lasers, inherently narrow linewidth [8–10]. However, because of the high spatial and temporal coherence of the laser sources, care has to be taken to avoid errors attributable to the interference arising from the reflections between parallel surfaces inside the filter radiometer [10].

In this study, two independent laser-based spectral irradiance responsivity calibration methods have been compared in the near-infrared wavelength region using a narrowband filter radiometer, FR800AR, as an artifact. The measurement facilities are at the NIST in the United States and at the Metrology Research Institute of the Helsinki University of Technology (TKK) in Finland, thus having completely independent traceability chains from the two inde-

0003-6935/07/204228-09$15.00/0

pendent primary standard cryogenic radiometers at the two facilities. Wavelength-tunable Ti:sapphire lasers are used at both facilities as the light sources and calibrated trap detectors as the reference standards for spectral power responsivity. However, the method for generating the uniform monochromatic irradiance is completely different. The SIRCUS facility at the NIST uses an integrating sphere to generate a uniform irradiance field [9] while the Laser Scanning Facility (LSF) at TKK [10] is based on the raster scanning technique using a single collimated laser beam; the effective irradiance is determined by calculation. Earlier comparisons of different calibration methods of spectral irradiance responsivity have revealed deviations, which have exceeded the stated uncertainties [11,12]. One reason for these discrepancies has been reported to have been higher than expected uncertainties in the wavelength scales at the comparison laboratories [12]. From this point of view, the laser-based calibration methods are likely to be more exact because of the ability for accurate real-time wavelength monitoring. In addition, different methods for minimization of the effect of the interference fringes, the observation of which is related to the use of monochromatic narrowband laser sources, are used in these facilities. The methods are compared and discussed along with the results obtained at the NIST Spectral Comparator Facility (SCF) [6] using a conventional monochromator-based light source.

In Section 2, the operational principles of the calibration facilities are explained. In Section 3, the construction of the measurement artifact is described, and the experimental procedure on each facility is presented. In Section 4, the uncertainty budgets for the measurement facilities are given. Section 5 presents the calibration results obtained with different methods. In Section 6, the implications of this study for applications in radiation thermometry and in photometry are discussed.

2. Description of the Facilities

In this section we briefly discuss the operational principles of each facility. The detailed descriptions of the SIRCUS, the LSF, and the SCF are found in [9], [10], and [6], respectively.

A. NIST SIRCUS Facility

In the SIRCUS facility, shown schematically in Fig. 1, high-power, tunable lasers are introduced into an integrating sphere producing a uniform, quasi-Lambertian, high radiant flux source. The laser beam is first directed through an intensity stabilizer that controls the relative optical power to within 0.01% of the set point. A portion of the laser beam is sent into a wavemeter that measures the wavelength of the radiation to within 0.001 nm. A beam splitter sends another portion of the laser beam into a Fabry–Perot interferometer to measure the bandwidth and mode stability of the laser. Finally, the laser radiation is introduced into an integrating sphere, often using an optical fiber [9]. Occasionally, a collimator coupled to

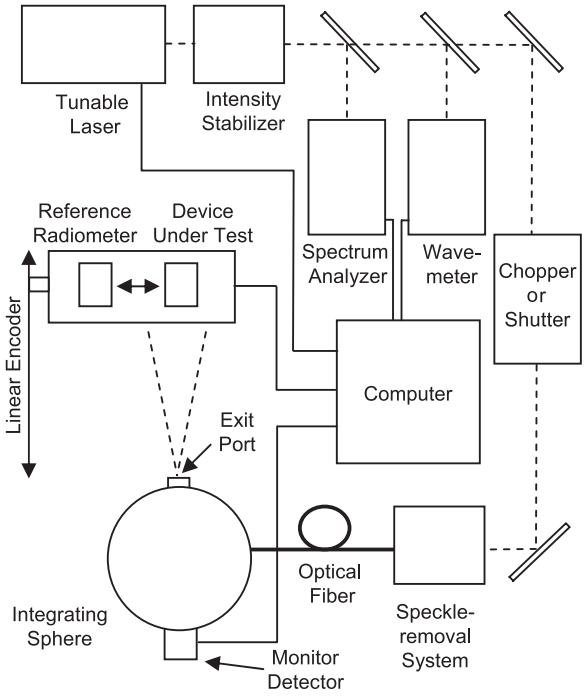

Fig. 1. Schematic of the SIRCUS facility at NIST.

the sphere is used as a calibration source. Speckle in the image from the source, originating from the coherent nature of the laser radiation, is effectively removed by either rastering the beam inside the sphere with a galvanometer-driven mirror or by placing a short length of optical fiber in an ultrasonic bath, thereby mixing the spatial modes in the fiber and the spatial distribution of the light from the fiber that hits the sphere wall.

Reference standard irradiance detectors, calibrated directly against national primary standards for spectral power responsivity [13] and equipped with a precision aperture measured on the NIST Aperture Area facility [14], are used to determine the irradiance at a reference plane. The source irradiance can be readily determined from the measurement geometry as well, which is necessary when the reference plane of the instrument being calibrated and that of the reference standard detector cannot be matched. A monitor photodiode is located on the sphere to correct for any radiant flux changes in the sphere output between measurements with the reference instrument and the device under test (DUT). The sources are located inside a lighttight box. Two baffles are typically installed between the source and the detectors to minimize effects of stray radiation on the measurement.

There are two separate SIRCUS facilities; the UV/Vis/NIR SIRCUS and the IR SIRCUS. The UV/Vis/NIR SIRCUS covers the range from 200 nm to 1.6 μm while the IR SIRCUS facility covers the spectral region from 780 nm to 5 μm. There is some overlap between the two facilities for scale intercomparisons. The two facilities are very similar; the main distinction is in the laser source used to illuminate the integrating spheres and the reference transfer

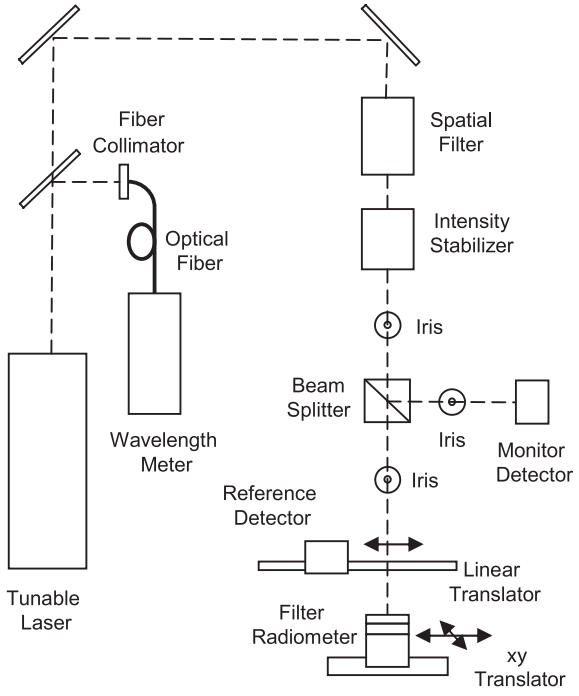

Fig. 2. Schematic of the Laser Scanning Facility at TKK.

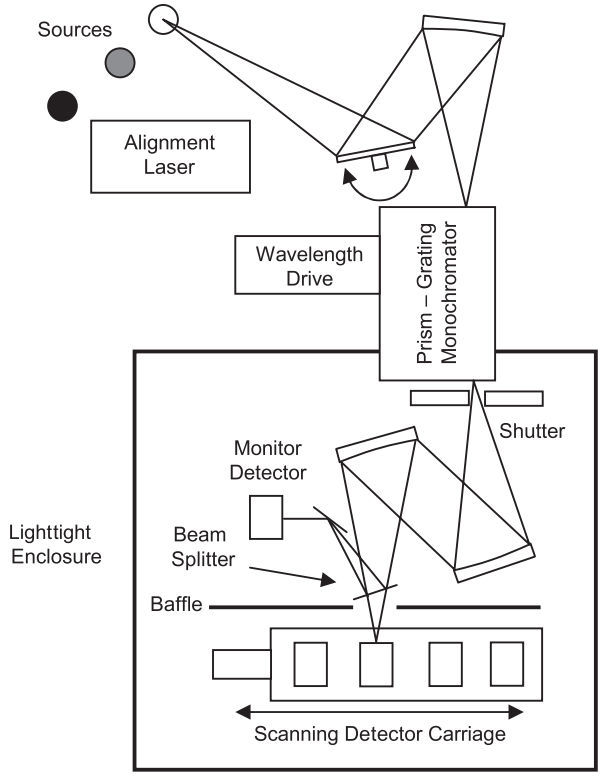

Fig. 3. Schematic of the Visible to Near-Infrared Spectral Comparator Facility at the NIST.

standards used to determine the irradiance at a reference plane. The UV/Vis/NIR SIRCUS was exclusively used in the comparison presented in this paper.

B. TKK Laser Scanning Facility

Figure 2 shows the schematic diagram of the LSF at TKK. The output from a wavelength-tunable cw Ti:sapphire laser is attenuated with a neutral density filter after which it is spatially filtered, collimated, and intensity stabilized. Part of the beam is directed to an optical wavelength meter for real-time wavelength monitoring. The uncertainty of the wavelength scale is estimated to be 0.003 nm. The spectral irradiance responsivity of the filter radiometer, $S(\lambda)$, is obtained by moving the filter radiometer with a high-accuracy translation stage step by step relative to the monochromatic laser beam and measuring the resulting photocurrent $I_{j,k}$ at each point [15]. The irradiance responsivity is then calculated by summing the signals measured, multiplying by the step sizes, and dividing by the incident power as

$$S(\lambda) = \frac{\sum_{j=1}^{n_x} \sum_{k=1}^{n_y} I_{j,k} \Delta x \Delta y}{P_L}. \quad (1)$$

In Eq. (1), n_x and n_y are the numbers of measurement points in the horizontal and vertical directions, Δx and Δy are the horizontal and vertical distances between the measurement points, and P_L is the power of the laser beam. The beam power is measured by moving a reference trap detector in front of the filter radiometer before and after each measurement of $S(\lambda)$. Part of the beam is directed to a monitor detector. During the scanning measurements, the photocurrents of the filter radiometer and the monitor detector are measured simultaneously to reduce the effects of remaining beam power fluctuations. Iris diaphragms are used to reduce stray light and back reflections. The dark currents of the detectors are also measured for the determination of $I_{j,k}$.

C. NIST Spectral Comparator Facility

The Visible to Near-Infrared Spectral Comparator Facility (Vis/NIR SCF) [6] is a monochromator-based system that measures the spectral radiant power responsivity of photodetectors in the 350–1800 nm spectral region as shown in Fig. 3. The main component of the Vis/NIR SCF is a prism-grating monochromator. The monochromator entrance slit is illuminated by a 100 W quartz halogen lamp. The typical exit aperture is a 1.1 mm diameter circular aperture, which is imaged ($\approx f/9$) onto the detectors. The bandwidth of the monochromator is 4 nm. A shutter is located just after the exit slit. A pair of orthogonal linear positioning stages translates the test detectors and the working standards. The detectors and the exit optics are enclosed in a lighttight box. The spatial uniformity of the detector responsivity can also be measured at any wavelength from 350 to 1800 nm.

3. Experimental Procedure

The calibration measurements were performed between November 2005 and March 2006. The mea-

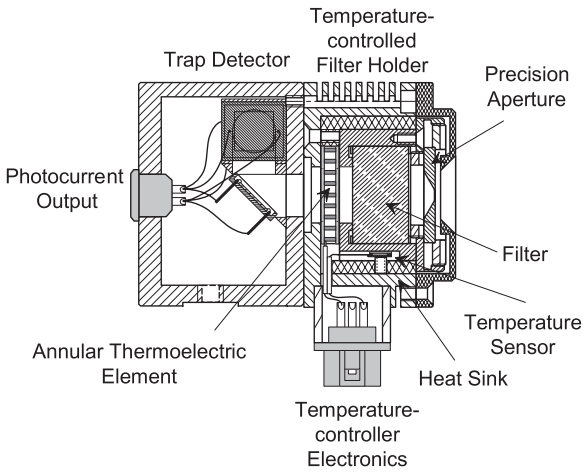

Fig. 4. Schematics of the filter radiometer FR800AR (picture reproduced from [12]).

surement artifact was first calibrated on SIRCUS and on the SCF at the NIST after which it was shipped to TKK for calibration on the LSF.

A. Description of the Measurement Artifact

The filter radiometer, FR800AR, was constructed at TKK and is similar in structure to the filter radiometers presented in [12]. A schematic view of the filter radiometer is shown in Fig. 4. It consists of a precision aperture with a nominal diameter of 3 mm, a bandpass interference filter with an effective central wavelength of 801 nm and a bandwidth of 24 nm (FWHM), and a three-element silicon trap detector. The temperature of the aperture and the filter was stabilized to (25 ± 0.5) °C by a thermoelectric cooling–heating system. The interference effect arising from inter-reflections of the coherent laser light between the layered structures of the filter was minimized by using a filter with slightly wedged surfaces and by applying an antireflection coating on the front surface of the filter. To compare the calibration methods, the spectral irradiance responsivity of FR800AR was measured with each method over a range of 33 nm around the bandcenter wavelength.

B. Measurements on SIRCUS

The spectral irradiance responsivity of the filter radiometer was calibrated on the SIRCUS utilizing the procedure described below. The measurements were made with average spectral intervals of 0.02 nm over the calibration range.

The entire data collection sequence on SIRCUS is automated. Initially, an electronic shutter that blocks the laser radiation before it enters the optical fiber is closed, and a background signal is acquired for both the reference standard trap detector and the sphere monitor. Then the shutter opens and the signals from the trap and the monitor on the sphere are recorded. The signals are initially amplified using a current-to-voltage amplifier and then fed into a digital voltmeter set to average over some number of power line cycles (the signal is averaged for a few seconds at most). Typically three shutter-closed signals and nine shutter-open signals are averaged. The mean reference-to-monitor ratio and the standard deviation of the ratio are recorded. After this, the stage moves to the DUT position, and the data acquisition sequence is repeated. This gives the DUT mean signal-to-monitor ratio and the standard deviation of the ratio. The standard deviations of the ratios are monitored; trap-detector-measurement standard deviations larger than 0.01% are an indication of laser power instabilities.

Under routine calibration conditions, the intensity-stabilized laser wavelength is read by the wavemeter and transferred to the computer during each measurement. Along with mean ratios, the mean and standard deviations of the wavelength are recorded. This enables ready identification of laser wavelength instabilities during a scan. Occasionally, for faster data acquisition, the wavelength is recorded only at the beginning of the acquisition sequence. Following the data acquisition sequence, the wavelength is changed and the sequence is repeated.

C. Measurements on the Laser Scanning Facility and Study of Interference Effects

The spectral irradiance responsivity of the filter radiometer was calibrated at the LSF by making measurements with spectral intervals of exactly 1 nm over the measurement range. The power of the laser beam was set to approximately 100 μW, and the $1/e^2$ diameter of the beam was approximately 3 mm. Step sizes of $\Delta x = 0.5$ mm and $\Delta y = 0.5$ mm and 15 measurement points for both the x and y directions were used as scanning parameters. Before the measurements, the FR800AR was carefully aligned perpendicular to the laser beam. Spurious reflections were eliminated by slightly tilting the optical components in front of the filter radiometer and monitoring the reflections using a CCD camera.

The effect of interference inside the filter radiometer gave rise to responsivity oscillation, as a function of laser wavelength, whose period was approximately 0.15 nm and the amplitude approximately 0.3% of the absolute responsivity when measured near the maximum of the responsivity curve. To compensate for this interference effect, oscillation patterns around every measurement point were determined by making relative responsivity measurements with spectral intervals of 0.02 nm over a full period of oscillation. The measured patterns were then fitted to the responsivity curve obtained from the absolute scanning measurements, and the absolute irradiance responsivity values at the measurement points were corrected to correspond to the average of the surrounding oscillation pattern. The method of least squares was used when fitting the data.

Because of the 10–15 min duration of the raster scanning measurements, relative measurements using a single laser beam rather than absolute scanning measurements were used in the determination of the

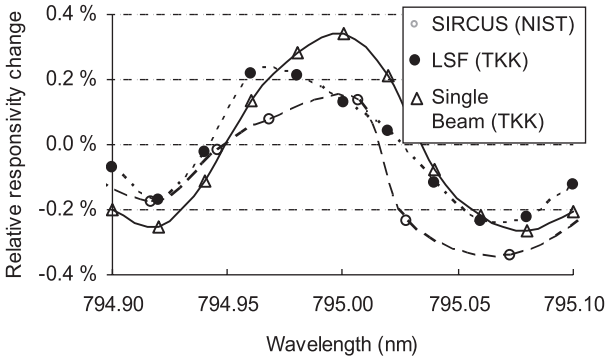

Fig. 5. Interference pattern measured close to 795 nm on SIRCUS, LSF, and with the single beam technique (see text).

oscillation pattern. The applicability of the single-beam method was confirmed by measuring a period of an oscillation pattern with single beam and raster scanning techniques. Figure 5 shows the result of such a measurement at approximately 795 nm together with the result from SIRCUS. In Fig. 5 the average value of the data obtained with the single-beam measurements is fixed to be the same as the average of absolute LSF raster scanning measurements. The results from the SIRCUS measurements share the same absolute scale with the raster scanning data, thus the true difference between these measurements can be evaluated. From Fig. 5 it is seen that, with the exception of a few measurement points, single-beam measurements match well with the raster scanning measurements, thus justifying the technique for oscillation pattern determination. Also, the results of the SIRCUS measurements are well in compliance with raster scanning measurements.

D. Measurements on the Spectral Comparator Facility

The spectral radiant power responsivity of the filter radiometer was determined over the measurement range in 1 nm wavelength increments by direct substitution comparisons to the silicon photodiode working standards. The effective aperture area of the filter radiometer was determined by scanning the monochromator output beam over the radiometer's entrance aperture in 0.125 mm increments to simulate a uniform irradiance. This method has been used by the NIST since 1991 [16]. The effective aperture area is proportional to the ratio of the total integrated signal of the scanned area and the signal from the center position. The spectral irradiance responsivity is the product of the spectral power responsivity and the effective aperture area [17].

4. Facility Uncertainty

This section summarizes the uncertainty budgets of each facility and the origins of the main uncertainty components. It should be noted that wavelength uncertainties are not included in the uncertainty budgets of SIRCUS and LSF because the effects of wavelength deviations are compared via the effective wavelength measurements.

Table 1. Uncertainty Budget of SIRCUS (NIST)

Source of Uncertainty	Relative Standard Uncertainty $\times 10^{-4}$
Reference detector responsivity	
Radiant power responsivity (400–920 nm)	2.5
Aperture area	0.4
Response uniformity	0.5
Cosine dependence	1.0
Temperature	0.3
Source characteristics	
Radiant flux	0.5
Irradiance uniformity	0.5
Determination of the reference plane	1.0
I-V Gain	1.0
Voltmeter reading	0.5
Transfer to device under test (estimated)	3.0
Temperature instability of device under test	2.8
Combined standard uncertainty	5.2

A. SIRCUS

The SIRCUS uncertainty budget is given in Table 1. Reference standard tunnel trap detectors hold the spectral irradiance responsivity scale on SIRCUS. The relative combined standard uncertainty in the detector responsivity is 2.5×10^{-4} at approximately 800 nm. To propagate the low uncertainties in power responsivity to irradiance responsivity, the detector's spatial response uniformity must be measured as well as the area of the defining aperture. The relative standard uncertainty of the area determination for a 5 mm diameter aperture is 4×10^{-5}. The response of a reference trap detector was found to be uniform to within 5×10^{-5} over the entire area of the entrance window (with the aperture removed). The uncertainty attributable to the responsivity deviation from the cosine function is 1×10^{-4} within a 6° field of view (FOV).

The radiant power uncertainty attributable to source instability is 5×10^{-5}. The irradiance is uniform to within 1×10^{-3} over the central ± 2 cm in both the horizontal and vertical directions, resulting in an uncertainty component of 5×10^{-5} attributable to irradiance uniformity in filter radiometer calibration. Given a 50 μm uncertainty in the trap reference plane, the uncertainty in the irradiance at a given reference plane for distances of 1 m or greater is 1×10^{-4}. The uncertainty of the current-to-voltage (I–V) conversion was 1×10^{-4} for gain selections between 10^4 V/A and 10^7 V/A. The estimated uncertainty in the transfer to the filter radiometer is listed in Table 1 as 3×10^{-4}. We have also included a term from the estimated uncertainty arising from temperature fluctuations. Taking the root-sum square of the individual uncertainty components, the combined

Table 2. Uncertainty Budget of LSF (TKK)

Source of Uncertainty	Relative Standard Uncertainty $\times 10^{-4}$
Irradiance	
Power of the laser beam	6.5
Step size of the *xy* translator	1.0
Interference effect	5.0
Temperature	2.8
Photocurrent of the filter radiometer	1.7
Combined standard uncertainty	8.9

relative standard uncertainty for the SIRCUS measurements is 5.2×10^{-4}.

B. Laser Scanning Facility

The summary of the relative combined standard uncertainty for the LSF facility is given in Table 2 according to the estimation presented in [10]. The main uncertainty components arise from the calibration of the power responsivity of the reference trap detector against the cryogenic radiometer (6.5×10^{-4}), from the interference effect inside the filter (5×10^{-4}), and from the temperature instability of the filter radiometer (2.8×10^{-4}). The fact that the filter radiometer was not tilted with respect to the laser beam, but other means were used for the elimination of spurious reflections, led to the exclusion of the uncertainty components related to the tilt of the radiometer reported earlier [10]. The combined relative standard uncertainty for the LSF is approximately 8.9×10^{-4}.

C. Spectral Comparator Facility

The uncertainty budget of the SCF at 800 and 818 nm is shown in Table 3. The former wavelength (800 nm) corresponds to the peak of the filter transmittance and the latter wavelength (818 nm) is located at the higher end of the measured wavelength range. The largest uncertainty components are attributable to the irradiance scanning calibration method, wavelength determination, and repeatability. Smaller uncertainty components are caused by amplifier gains, digital voltmeter, and stray light.

Table 3. Uncertainty Budget of SCF (NIST)

Source of Uncertainty	Relative Standard Uncertainty $\times 10^{-4}$ 800 nm	818 nm
Repeatability and random noise	2	46
Irradiance method (scanning)	58	58
Working standard calibration	9	9
Working standard amplifier gain	4	4
Test detector amplifier gain	4	4
Voltmeter reading	1	1
Wavelength ($\pm$0.1 nm)	3	415
Spectral stray light	0	2
Combined standard uncertainty	59	422

The combined standard uncertainty is 59×10^{-4} at 800 nm and 422×10^{-4}, at 818 nm. The relatively high value of uncertainty at 818 nm is attributable mainly to the uncertainty in the wavelength determination, which causes high uncertainty when measuring at the regions where the transmittance of the filter changes rapidly as a function of the wavelength.

5. Results

The absolute spectral irradiance responsivity curves of the FR800AR obtained with the three methods are plotted over the entire measurement range on a logarithmic scale in Fig. 6(a) and close to the responsivity maximum on a linear scale in Fig. 6(b). The irradiance responsivity curves obtained with the two laser-based methods are in good agreement with each other. It should be noted that the LSF points plotted in Fig. 6 represent the interference-corrected values, i.e., values that are spectrally averaged over the surrounding interference cycle, while the SIRCUS points represent absolutely measured values at each wavelength. The shape of the responsivity curve obtained from the measurements on SCF is highly affected by the large bandwidth of the source, which makes the individual measurement points represent values that are spectrally averaged over several nanometers. Therefore the SCF data deviates significantly from the other two data sets and cannot be directly compared with them at precise wavelengths.

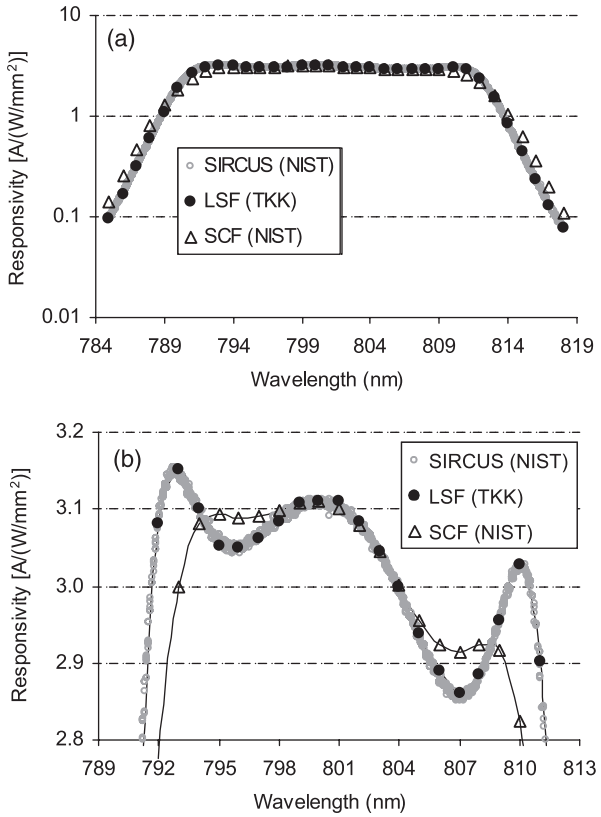

Fig. 6. Spectral irradiance responsivity of the filter radiometer measured on SIRCUS, LSF, and SCF (a) over the entire measurement range, (b) close to the responsivity maximum.

Table 4. Integrated Irradiance Responsivity of FR800AR[a]

	Integrated Response [A/(W/mm^2) nm]	Relative Standard Uncertainty $\times 10^{-4}$	Relative Difference to Weighted Average $\times 10^{-4}$
SIRCUS (NIST)	72.830	5.2	−1.0
LSF (TKK)	72.859	8.9	3.0
SCF (NIST)	72.833	59	−0.6

[a]The data were calculated over the wavelength range 785–818 nm from the results of spectral irradiance calibrations on SIRCUS, LSF, and SCF. The corresponding relative standard uncertainties are shown and the results are compared to the weighted average of all the methods.

The agreement between the calibration methods was evaluated by calculating the integrated response [12]

$$S = \int_{785\ \mathrm{nm}}^{818\ \mathrm{nm}} S(\lambda)\mathrm{d}\lambda \tag{2}$$

for spectral responsivity results over the calibration range. The integrated responses corresponding to each calibration are given in Table 4 and are compared with the weighted average of the results calculated as

$$\bar{S} = \frac{\sum_{i=1}^{3} S_i u_i^{-2}}{\sum_{i=1}^{3} u_i^{-2}}, \tag{3}$$

where S_i are the integrated responses obtained from the three different calibrations, and parameters u_i are the corresponding standard uncertainties. The integrated responsivity values for all compared methods are well within the stated standard uncertainties.

The effective wavelength values

$$\lambda_{eff} = \frac{\int_{785\ \mathrm{nm}}^{818\ \mathrm{nm}} \lambda S(\lambda)\mathrm{d}\lambda}{\int_{785\ \mathrm{nm}}^{818\ \mathrm{nm}} S(\lambda)\mathrm{d}\lambda}, \tag{4}$$

for each calibration were calculated to reveal possible discrepancies in the determinations of the wavelength scales between different methods. The results are presented in Table 5 and are compared with the weighted average of the results calculated as

$$\bar{\lambda}_{eff} = \frac{\sum_{i=1}^{3} \lambda_{eff_i} w_i^{-2}}{\sum_{i=1}^{3} w_i^{-2}}, \tag{5}$$

where λ_{eff_i} are the effective wavelengths obtained from the three different calibrations, and parameters w_i are the corresponding standard uncertainties. The effective wavelengths given by the laser-based calibrations match well with each other. The results are within the stated expanded ($k = 2$) uncertainties of 0.002 nm for SIRCUS and 0.006 nm for the LSF. The effective wavelength extracted directly from the SCF calibration is also in agreement with the other two, deviating 0.016 nm from the weighted average, but its expanded uncertainty of 0.2 nm is approximately 2 orders of magnitude higher compared to the uncertainties of the laser-based methods. The effect of convolution, attributable to the broad spectral width of the source, causes a slight wavelength shift in the SCF data. This can be compensated by deconvolving the data using the monochromator's slit function. It is estimated that the deconvolution would cause approximately a 0.01 nm shift to the SCF effective wavelength.

Table 5. Effective Wavelength of FR800AR[a]

	Effective Wavelength [nm]	Standard Uncertainty [nm]	Difference to Weighted Average [nm]
SIRCUS (NIST)	801.194	0.001	0.001
LSF (TKK)	801.187	0.003	−0.006
SCF (NIST)	801.209	0.1	0.016

[a]The data calculated over the wavelength range 785–818 nm from the results of spectral irradiance calibrations on SIRCUS, LSF, and SCF. The corresponding standard uncertainties are shown, and the results are compared to the weighted average of all the methods.

6. Discussion

Both laser-based methods in this study are based on a wavelength-tunable Ti:sapphire laser. The main difference between the methods lies in the mechanism by which a uniform irradiance is generated from the laser source. On SIRCUS, integrating spheres with a precision aperture are employed, while on LSF the uniform irradiance is generated using the raster scanning technique. The advantage of the raster scanning technique is that it removes the need for the determination of the distance between the source and the detector, which is needed on SIRCUS when the reference plane of the instrument being calibrated and that of the reference detector cannot be matched. On the other hand, the time needed for a scan measurement is relatively long, which restricts the number of measurement points. This has an impact on how the effect of interference is treated. On SIRCUS it is possible to measure the whole band with a spectral resolution good enough to follow the interference pattern continuously. On the LSF, in contrast, the

interference effect is taken into account by determining the interference pattern around every measurement point and calculating a correction factor for every measurement point. In any case, care has to be taken when designing the filter radiometer to minimize interference effects, for example, by the use of wedged optical elements and antireflection coatings.

The results of this comparison have implications for a number of radiometric applications where high-accuracy spectral radiance and irradiance measurements are crucial. In one example, the uncertainty in an absolute detector-based radiometric temperature scale, studied extensively at different NMIs [11,18–20] depends mostly on the accuracy of the NMIs spectral radiance and irradiance responsivity scales. The freezing temperatures of gold, silver, and aluminum fixed points, defined by the International Temperature Scale of 1990 (ITS-90) [21], have been measured by using radiometric detectors traceable to absolute cryogenic radiometers, with uncertainties similar to the thermodynamic measurements of temperature reported in the ITS-90 [18,19]. However, before the detector-based radiometric temperature scales can be considered as suitable alternatives to the relative fixed-point-based method of ITS-90, more studies on the reliability of these different detector-based methods have to be conducted. While in most of the radiometric temperature measurements radiometers that measure the radiance of blackbody sources are used, the spectral irradiance measurements are usually an essential part of their spectral radiance responsivity calibration [9]. Significant improvements in the spectral irradiance scales have been made, especially in the shortwave IR region [3,4].

For temperatures above the freezing temperature of silver, the ITS-90 is defined in terms of spectral radiance ratios of the silver-, gold- or copper-freezing temperature blackbodies using the Planck radiance law. In the ITS-90, the assigned temperatures for the Ag, Au, and Cu freezing points result from thermometry using ratio pyrometry from the mean of two different and conflicting constant-volume gas thermometry measurements at lower temperatures. There are thermodynamic temperature uncertainties of the freezing points of the primary metal blackbodies that arise primarily from the uncertainties in the lower-temperature gas thermometry. Because of the use of spectral radiance ratios, the temperature uncertainties of the ITS-90 assigned blackbodies, $u(T_{BB})$, increase as the square of the temperature ratios according to

$$u(T_{BB}) = \frac{u(T_{FP})}{{T_{FP}}^2}\,{T_{BB}}^2, \tag{6}$$

where T_{FP} and $u(T_{FP})$ are the temperature and the uncertainty of the fixed-point blackbody, and T_{BB} is the temperature of the higher-temperature blackbody. The increases in the temperature uncertainties can be reduced by using absolute radiometry with pyrometers traceable to cryogenic radiometers, and the resulting temperature uncertainties can be smaller than those measured using the ITS-90 techniques [22].

The results of this comparison may also have implications in photometry. The redefinition of the candela in 1979 coupled photometric and radiometric units [23] and made it possible to realize and maintain photometric units using detectors as well as sources. Following the redefinition, many NMIs, including TKK and the NIST, derive and maintain the candela (and the derived photometric units) by using calibrated standard detectors traceable to cryogenic radiometers [24,25] rather than standard lamps traceable to primary standard blackbodies and international temperature scales. By using tunable lasers to measure the spectral responsivity of photometers, the present uncertainties, at the 0.5% level [26] may be reduced to approximately 0.1%, primarily because of the improved accuracy of the wavelength scale. In this case, the uncertainty budget may be dominated by the radiometric stability of the instrument (filter and detector) not the calibration itself.

7. Conclusions

In this paper, we have presented the results of a study of two laser-based calibration methods for absolute spectral irradiance responsivity in the near-infrared wavelength region. A narrow bandwidth filter radiometer was calibrated as an artifact on two National Metrology Institutes' laser-based calibration facilities, on SIRCUS at the NIST and on the LSF at TKK. A calibration was also performed on the NIST SCF to compare laser-based methods with a conventional monochromator-based method. The agreement between the methods was evaluated with respect to the integrated irradiance responsivities and effective wavelengths calculated from the calibration data.

The results of all three methods were found to agree with each other in terms of the integrated responsivities within the limits of stated uncertainties, the laser-based methods offering significantly lower uncertainties than the monochromator-based method. The study of the effective wavelength values showed that the wavelength scales used on SIRCUS and LSF match quite well with each other. The spectral averaging attributable to the broad spectral width of the monochromator source causes a slight wavelength shift in the SCF data. However, the difference between the effective wavelengths extracted from the SCF data and from the average of the laser-based methods is well within the expanded ($k = 2$) uncertainty of the SCF wavelength scale.

This study has validated the stated low uncertainties, somewhat below 0.1% ($k = 1$), of the studied laser-based spectral irradiance calibration methods in the near-infrared region. The study also showed that the wavelength scale for the calibration can be realized with high accuracy using laser-based methods. As explained in Section 6, the results are significant for applications in radiation thermometry as well as in photometry.

References

1. V. E. Anderson and N. P. Fox, "A new detector-based spectral emission scale," Metrologia **28,** 135–139 (1991).
2. P. Sperfeld, K.-H. Raatz, B. Nawo, W. Möller, and J. Metzdorf, "Spectral-irradiance scale based on radiometric blackbody temperature measurements," Metrologia **32,** 435–439 (1996).
3. T. Kübarsepp, P. Kärhä, F. Manoocheri, S. Nevas, L. Yliantila, and E. Ikonen, "Spectral irradiance measurements of tungsten lamps with filter radiometers in the spectral range 290 nm to 900 nm," Metrologia **37,** 305–312 (2000).
4. H. W. Yoon, C. E. Gibson, and P. Y. Barnes, "Realization of National Institute of Standards and Technology detector-based spectral irradiance scale," Appl. Opt. **41,** 5879–5890 (2002).
5. M. Durak and F. Samadov, "Realization of a filter radiometer-based irradiance scale with high accuracy in the region from 286 nm to 901 nm," Metrologia **41,** 401–406 (2004).
6. T. C. Larason, S. S. Bruce, and A. C. Parr, *Spectroradiometric Detector Measurements: Part I–Ultraviolet Detectors and Part II–Visible to Near-Infrared Detectors,* Natl. Inst. Stand. Technol. Spec. Publ. 250-41 (U.S. Government Printing Office, 1998).
7. P. Kärhä, A. Haapalinna, P. Toivanen, F. Manoocheri, and E. Ikonen, "Filter radiometry based on direct utilization of trap detectors," Metrologia **35,** 255–259 (1998).
8. V. E. Anderson, N. P. Fox, and D. H. Nettleton, "Highly stable, monochromatic and tunable optical radiation source and its application to high accuracy spectrophotometry," Appl. Opt. **31,** 536–545 (1992).
9. S. W. Brown, G. P. Eppeldauer, and K. R. Lykke, "Facility for spectral irradiance and radiance responsivity calibrations using uniform sources," Appl. Opt. **45,** 8218–8237 (2006).
10. M. Noorma, P. Toivanen, F. Manoocheri, and E. Ikonen, "Characterization of filter radiometers with a wavelength-tunable laser source," Metrologia **40,** S220–S223 (2003).
11. H. W. Yoon, P. Sperfeld, S. Galal Yousef, and J. Metzdorf, "NIST-PTB measurements of the radiometric temperatures of a high-temperature blackbody using filter radiometers," Metrologia **37,** 377–380 (2000).
12. P. Kärhä, N. J. Harrison, S. Nevas, W. S. Hartree, and I. Abu-Kassem, "Intercomparison of characterization techniques of filter radiometers in the ultraviolet region," Metrologia **40,** S50–S54 (2003).
13. J. M. Houston and J. P. Rice, "NIST reference cryogenic radiometer designed for versatile performance," Metrologia **43,** S31–S35 (2006).
14. J. Fowler and M. Litorja, "Geometric area measurements of circular apertures for radiometry at NIST," Metrologia **40,** S9–S12 (2003).
15. P. Toivanen, F. Manoocheri, P. Kärhä, E. Ikonen, and A. Lassila, "Method for characterization of filter radiometers," Appl. Opt. **38,** 1709–1713 (1999).
16. J. M. Bridges and C. L. Cromer, *Final Report on Calibration and Characterization of I-Line Exposure Meters,* Report 91 090 678A-ENG (International SEMATECH, Austin, Tex., USA, 1991).
17. G. P. Eppeldauer, M. Racz, and T. C. Larason, "Optical characterization of diffuser-input standard irradiance meters," Proc. SPIE **3573,** 220–224 (1998).
18. N. P. Fox, J. E. Martin, and D. H. Nettleton, "Absolute spectral radiometric determination of the thermodynamic temperatures of the melting/freezing points of gold, silver and aluminium," Metrologia **28,** 357–374 (1991).
19. H. W. Yoon, C. E. Gibson, D. W. Allen, R. D. Saunders, M. Litorja, S. W. Brown, G. P. Eppeldauer, and K. R. Lykke, "The realization and dissemination of the detector-based kelvin," in *Proceedings of Tempmeko 04* (Dubrovnik, 2004), pp. 59–70.
20. M. Noorma, P. Kärhä, T. Jankowski, F. Manoocheri, T. Weckström, L. Uusipaikka, and E. Ikonen, "Absolute detector-based radiometric temperature scale," in *Proceedings of Tempmeko 04* (Dubrovnik, 2004), pp. 101–106.
21. H. Preston-Thomas, "The international temperature scale of 1990 (ITS-90)," Metrologia **27,** 3–10 (1990).
22. H. W. Yoon, D. W. Allen, C. E. Gibson, M. Litorja, R. D. Saunders, S. W. Brown, G. P. Eppeldauer, and K. R. Lykke, "Temperature determination of the Ag and Au freezing points using a detector-based radiation thermometer," in *Proceedings of Tempmeko 04* (Dubrovnik, 2004), pp. 113–118.
23. "Principles governing photometry," Metrologia **19,** 97–101 (1983).
24. P. Toivanen, P. Kärhä, F. Manoocheri, and E. Ikonen, "Realization of the unit of luminous intensity at the HUT," Metrologia **37,** 131–140 (2000).
25. Y. Ohno, "Improved photometric standards and calibration procedures at NIST," J. Res. Natl. Inst. Stand. Technol. **102,** 323–331 (1997).
26. R. Köhler, M. Stock, and C. Garreau, "Final report on the international comparison of luminous responsivity CCPR-K3.b," Metrologia **41,** Tech. Suppl. 02001 (2004).